Dalton Transactions

COMMUNICATION

View Article Online
View Journal

Cite this: DOI: 10.1039/c5dt04517g

Received 17th November 2015,
Accepted 1st December 2015

DOI: 10.1039/c5dt04517g

www.rsc.org/dalton

A novel method for the synthesis of solvent-free $Mg(B_3H_8)_2$†

Jianmei Huang,[a,b,c] Yigang Yan,*[c] Arndt Remhof,[c] Yucheng Zhang,[c] Daniel Rentsch,[c] Yuen S. Au,[d] Petra E. de Jongh,[d] Fermin Cuevas,[e] Liuzhang Ouyang,*[a] Min Zhu[a] and Andreas Züttel[b,c]

This communication presents a novel and solvent-free method to synthesise $Mg(B_3H_8)_2$ *via* the gas–solid reaction between B_2H_6 and Mg_2NiH_4, which overcomes the limitations of wet chemical methods requiring solvent removal.

Octahydrotriborate $[B_3H_8]^-$ is the third member of the hydroborate series after $[BH_4]^-$ and $[B_2H_7]^-$. It has been widely utilised as a precursor in chemical reactions such as the chemical vapour deposition (CVD) of metal-boride (*e.g.*, MgB_2 and CrB_2) thin films,[1,2] and the synthesis of higher boranes[3,4] or carborane cluster compounds.[5] Owing to their high hydrogen density, octahydrotriborates have also been discussed as hydrogen storage materials (*e.g.*, NaB_3H_8 and $NH_4B_3H_8$).[6,7] Recently, $[B_3H_8]^-$ compounds have received particular attention, as they were observed to be crucial intermediates in the decomposition of metal borohydrides, for example, $Mg(B_3H_8)_2$ in the case of $Mg(BH_4)_2$.[8–10] However, their roles in hydrogen sorption cycles have not been fully understood and their properties such as stability and reactivity are still unknown, owing to the challenge of synthesising compounds (*e.g.*, $Mg(B_3H_8)_2$) in a solvent-free state.

The preparation of solvent-free NaB_3H_8 has been reported previously.[11–14] A common synthetic route involves the use of Na/Hg amalgam, which reacts with either B_2H_6 or $THF{\cdot}BH_3$ to form NaB_3H_8, yielding $NaBH_4$ as a by-product.[11–13] By applying diethyl ether, insoluble $NaBH_4$ could be easily separated and $NaB_3H_8(THF)_x$ could be obtained when $THF{\cdot}BH_3$ was used; this complex can be de-solvated after breaking the coordination between THF and Na by adding CH_2Cl_2 followed by heating under vacuum. Attempts to synthesise $Mg(B_3H_8)_2$ have included the metathesis reaction of NaB_3H_8 and $MgBr_2$ in Et_2O or Me_2O as well as the reaction between Mg/Hg amalgam and $THF{\cdot}BH_3$.[1,15,16] Both methods resulted in the formation of complexes such as $Mg(B_3H_8)_2(Et_2O)_2$, $Mg(B_3H_8)_2(Me_2O)_2$, or $Mg(B_3H_8)_2(THF)_x$. However, the desolvation of these complexes led to the decomposition of $Mg(B_3H_8)_2$, owing to the strong coordination of Mg to the solvents.

Gas–solid reactions involving B_2H_6 have been used to synthesise metal borohydrides and metal dodecaborates.[9,17–20] $Mg(BH_4)_2$ was, for example, synthesised by reactive ball-milling of MgH_2 under B_2H_6 at room temperature.[17] Further exposure of $Mg(BH_4)_2$ to B_2H_6 at elevated temperature led to the formation of $MgB_{12}H_{12}$ through a B–H condensation process, in which $Mg(B_3H_8)_2$ was observed as a reaction intermediate.[18] The presence of metal particles, such as Ni particles, was reported to facilitate the splitting of B_2H_6.[21] In a recent study, the reaction between B_2H_6 and MgH_2 (average particle size 10 nm) at room temperature was found to be altered when Ni nanoparticles were present, whereby higher boranes such as $Mg(B_5H_8)_2$ were formed instead of $Mg(BH_4)_2$.[20]

Mg_2NiH_4 is an ionic hydride composed of Mg^{2+} and the complex anion $[NiH_4]^{4-}$.[22] In the present study, we found that the reaction between Mg_2NiH_4 and B_2H_6 readily occurs at room temperature, and the formation of $Mg(B_3H_8)_2$ is observed as shown in eqn (1). This finding provides a facile approach to the direct synthesis of solvent-free $Mg(B_3H_8)_2$.

$$Mg_2NiH_4 + 6B_2H_6 \rightarrow 2Mg(B_3H_8)_2 + Ni + 4H_2 \qquad (1)$$

The starting material, a composite of Mg_2NiH_4 and carbon aerogel in the mass ratio of 1 to 9 (denoted as Mg_2NiH_4/C), was prepared by high-energy ball milling (spex8000) under an argon atmosphere for 2 h. Sequentially, Mg_2NiH_4/C was directly exposed to B_2H_6 at room temperature for 3 days without applying additional ball-milling. Magnesium hydroborates such as $Mg(BH_4)_2$, $Mg(B_3H_8)_2$ and $MgB_{12}H_{12}$ have been

[a]*School of Materials Science and Engineering and Guangdong Provincial Key Laboratory of Advanced Energy Storage Materials, South China University of Technology, 510641 Guangzhou, China. E-mail: meouyang@scut.edu.ch*
[b]*Institute of Chemical Sciences and Engineering (ISIC), École polytechnique fédérale de Lausanne (EPFL) Valais/Wallis, Energypolis, 1950 Sion, Switzerland*
[c]*Empa-Swiss Federal Laboratories for Materials Science and Technology, 8600 Dübendorf, Switzerland. E-mail: yigang.yan@empa.ch*
[d]*Inorganic Chemistry and Catalysis, Debye Institute for Nanomaterials Science, Utrecht University, Universiteitsweg 99 3584 CG, Utrecht, The Netherlands*
[e]*CMTR/ICMPE/CNRS UMR 7182, 2-8 rue Henri Dunant, 94320 Thiais Cedex, France*

†Electronic supplementary information (ESI) available: Experimental details, ^{1}H-coupled ^{11}B NMR spectrum of the as synthesised $[B_3H_8]^-$ species, STEM-HAADF image, HRTEM image, B mapping signal and EELS (B) signal of Mg_2NiH_4/C ball milled under B_2H_6 for 24 h. See DOI: 10.1039/c5dt04517g

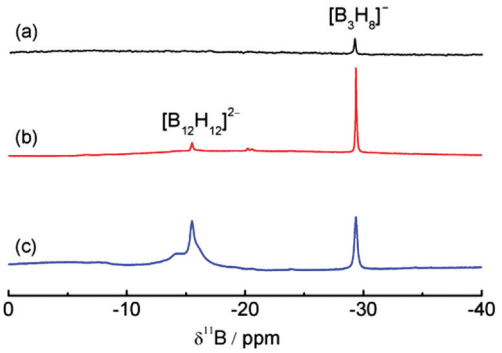

Fig. 1 $^{11}B\{^1H\}$ NMR spectra of DMSO-d_6 solutions of Mg_2NiH_4/C composites exposed to B_2H_6 at room temperature for (a) 3 days without additional ball-milling or (b) 6 h and (c) 24 h with additional ball-milling.

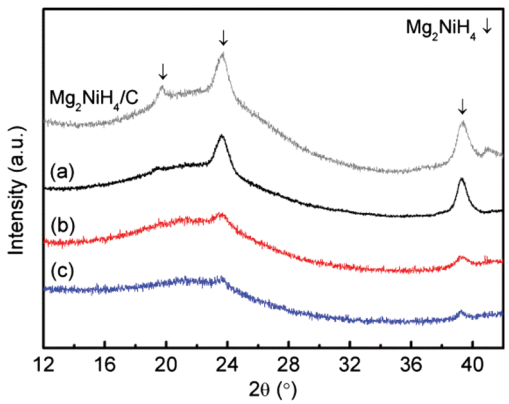

Fig. 2 XRD patterns of pristine Mg_2NiH_4/C and Mg_2NiH_4/C exposed to B_2H_6 at room temperature for (a) 3 days without additional ball-milling or (b) 6 h and (c) 24 h with additional ball-milling.

found to be fully soluble in DMSO, which was thereby used here to extract the newly formed Mg–B–H species for phase identification by solution-state ^{11}B nuclear magnetic resonance (NMR) measurements.[18,23] As shown in Fig. 1a, a new resonance at δ = −29.3 ppm, assigned to the $[B_3H_8]^-$ species, was observed in the DMSO-d_6 solution of the Mg_2NiH_4/C composite exposed to B_2H_6.[18] It showed a typical nonet splitting with a coupling constant of 33 Hz (Fig. S2†). No additional resonances assignable to side products such as $Mg(BH_4)_2$ were observed. The X-ray diffraction (XRD) pattern of this sample is shown in Fig. 2a. No obvious decrease in the reflection intensities of the Mg_2NiH_4 phase was observed after reaction with B_2H_6, indicating that the overall reaction yield of $Mg(B_3H_8)_2$ was limited.

The reaction rate between Mg_2NiH_4/C and B_2H_6 was increased by additional reactive ball-milling (low-energy) at room temperature.[17] After ball-milling for 6–24 h under a B_2H_6 atmosphere, the majority of the Mg_2NiH_4 phase (Fig. 2b and c) disappeared. Meanwhile, a much stronger $[B_3H_8]^-$ resonance was observed by using ^{11}B NMR (Fig. 1b), indicating an

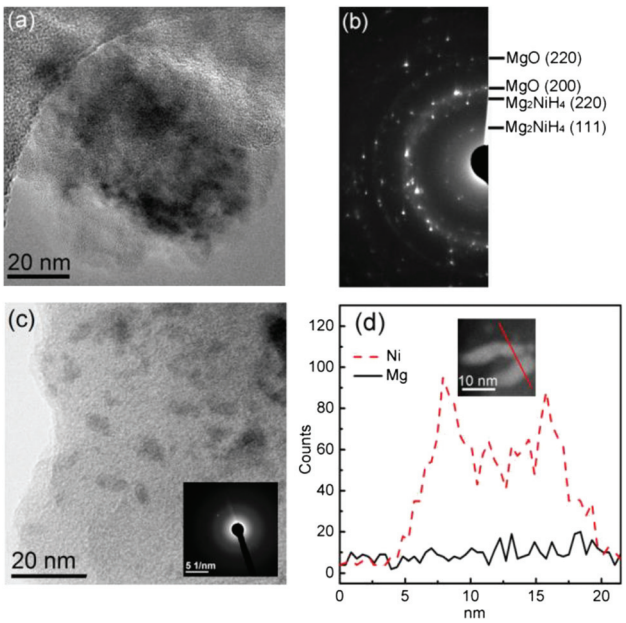

Fig. 3 (a) Bright-field TEM image and (b) SAED pattern of Mg_2NiH_4/C. The MgO phase originated from the oxidation of Mg_2NiH_4 during the sample loading process in air for measurements. (c) Bright-field STEM image and inserted SAED pattern of Mg_2NiH_4/C ball milled under B_2H_6 for 24 h. (d) STEM-EDS line profiles of Mg and Ni along the red line of the inserted STEM-HAADF image of selected nanoparticles in (c).

improvement in the yield of $Mg(B_3H_8)_2$ after ball-milling for 6 h. Additionally, a minor resonance at δ = −15.3 ppm assigned to $[B_{12}H_{12}]^{2-}$ was observed, which became stronger when ball-milling was performed for 24 h (Fig. 1c).

The morphologies of Mg_2NiH_4/C before and after the reaction with B_2H_6 were compared by means of transmission electron microscopy (TEM) and scanning TEM (STEM). Pristine Mg_2NiH_4/C showed aggregation of the Mg_2NiH_4 grains (Fig. 3a) with diffraction rings observed in the selected area electron diffraction (SAED) pattern (Fig. 3b), indicating the crystalline nature of the sample. After ball milling of Mg_2NiH_4/C under B_2H_6 for 24 h, the absence of lattice fringes (Fig. 3c and S3†) and the SAED pattern (the insert of Fig. 3c) indicated only the presence of an amorphous phase. This supports the conversion of crystalline Mg_2NiH_4 into an amorphous phase, which is in agreement with the XRD observations (Fig. 2b and c).

Furthermore, nanoparticles with sizes from 3 to 15 nm were detected after ball-milling of Mg_2NiH_4/C under B_2H_6 (Fig. 3c and S3†). To identify the newly-formed nanoparticles observed in Fig. 3c, a selected particle (the insert of Fig. 3d) was measured using an energy-dispersive X-ray spectroscopy (EDS) line scan, following the red line. Here, the bright area refers to Ni-containing particles with higher electron density, while the black area refers to compounds composed of more lightweight elements such as Mg, B, C and H. It was found that Mg showed a uniform distribution along the entire scanned line, whereas the distribution of Ni showed a strong

dependence on the position (Fig. 3d). The signal of Ni on the particle (bright area) was much stronger than that away from the particle (black area). Therefore, the newly formed nanoparticles (Fig. 3c) did contain Ni, but were not Mg-containing compounds (*e.g.*, not Mg_2Ni). To determine whether these nanoparticles were metallic Ni or Ni–B compounds, STEM high angle annular dark field (HAADF) imaging (Fig. S4a and b†), EDS mapping (Fig. S4c†) and electron energy loss spectroscopy (EELS) (Fig. S4d†) measurements were performed. In regions on the selected particle and away from the particle, no obvious difference was observed on both the intensity of the boron signal (Fig. S4c†) and the chemical shift of the B K-edge (Fig. S4d†). These observations implied the formation of amorphous Ni nanoparticles. However, it still cannot be ruled out that these amorphous particles are rich in Ni but contain a small amount of boron atoms forming as Ni_xB.[24]

We have shown that Mg_2NiH_4 readily reacts with B_2H_6 at room temperature to form $Mg(B_3H_8)_2$, according to eqn (1). By applying ball-milling, the reaction was faster and the majority of Mg_2NiH_4 was converted into $Mg(B_3H_8)_2$ within 6 h. Elongated ball milling resulted in further conversion of $Mg(B_3H_8)_2$ into $MgB_{12}H_{12}$. Ni was considered to be essential for the formation of $Mg(B_3H_8)_2$ in this study since no $Mg(B_3H_8)_2$ was formed through the reaction between MgH_2 and B_2H_6.[17] Also, due to the formation of paramagnetic Ni or Ni_xB particles after ball milling, the investigation of the yield of $Mg(B_3H_8)_2$ by solid-state ^{11}B NMR failed. Therefore a quantitative analysis based on solution-state ^{11}B NMR was conducted, using a DMSO-d_6 solution of $K_2B_{12}H_{12}$ (12 mM) as the external reference (shown in Fig. S5†). For the sample of Mg_2NiH_4/C after 6 h ball milling under B_2H_6, 10 mg of the sample was added to 3 mL of DMSO-d_6 and a 3.8 mM of $Mg(B_3H_8)_2$ and 0.27 mM of $MgB_{12}H_{12}$ solution was detected by ^{11}B NMR. The composition of this sample was thus determined as: 12.1 wt% $Mg(B_3H_8)_2$, 1.4 wt% $MgB_{12}H_{12}$, 3.9 wt% Ni (or Ni_xB), 6.8 wt% Mg_2NiH_4 residue, and 75.8 wt% carbon. The conversion ratio of Mg_2NiH_4 to $Mg(B_3H_8)_2$ was 74.5%. Owing to the high vapour pressure, $Mg(B_3H_8)_2$ could be evaporated from this mixture and collected in a cold trap. Further purification of $Mg(B_3H_8)_2$ and the study of its properties are in progress.

Further conversion of $Mg(B_3H_8)_2$ with B_2H_6 results in the formation of $MgB_{12}H_{12}$, according to eqn (2). This reaction path allows the synthesis of solvent-free $MgB_{12}H_{12}$, which was suggested to be a potential solid electrolyte for Mg batteries.[25]

$$Mg(B_3H_8)_2 + 3B_2H_6 \rightarrow MgB_{12}H_{12} + 11H_2 \quad (2)$$

Two reaction paths from Mg_2NiH_4 to $Mg(B_3H_8)_2$ could be considered:

(1) The reaction proceeds *via* the formation of an intermediate "$Mg(BH_4)_2$". The reaction process is depicted in Scheme 1. The Mg_2NiH_4 complex is composed of $2Mg^{2+}$ cations and $[NiH_4]^{4-}$ anions, in which each Ni atom is surrounded by four H^- in a tetrahedral configuration.[22] In the first step, H^- in $[NiH_4]^{4-}$ anions may combine with BH_3 provided by B_2H_6 and form $[BH_4]^-$, resulting in the decomposition of Mg_2NiH_4 and the formation of $Mg(BH_4)_2$ and Ni (or existing as Ni_xB).

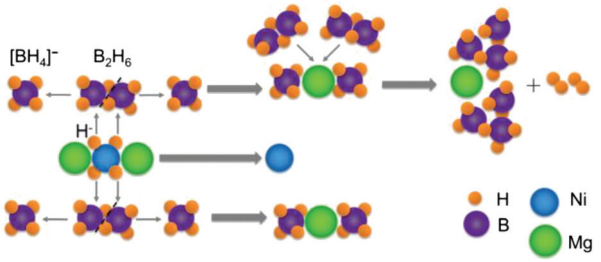

Scheme 1 Proposed mechanism of the reaction between Mg_2NiH_4 and B_2H_6 to form $Mg(B_3H_8)_2$ *via* the intermediate of $Mg(BH_4)_2$ at room temperature.

Adsorption and decomposition of B_2H_6 on the Ni(100) surface have been observed at low temperature.[26] Ni and Ni_xB were also reported to be catalysts to increase the reaction kinetics for boron-based hydrides during the hydrogen uptake process.[20,24,27,28] In the presence of *in situ* forming Ni (or Ni_xB) nanoparticles (3–15 nm), both the splitting of B_2H_6 into BH_3 units and the reaction between $Mg(BH_4)_2$ and BH_3 forming $Mg(B_3H_8)_2$ could be catalysed. The intermediate species "$Mg(BH_4)_2$" was not observed in our experiments, possibly owing to its short lifetime.

Note that there was 4 wt% Ni residual in the initial Mg_2NiH_4 sample, which may trigger the splitting of B_2H_6 and result in the reaction between B_2H_6 and Mg_2NiH_4 forming $Mg(B_3H_8)_2$ at room temperature without additional ball milling.

(2) The binding energy of Ni–H in Mg_2NiH_4 is much less than that of Mg–H in MgH_2.[29,30] $[NiH_4]^{4-}$ could donate H^- to B_2H_6 forming an intermediate, $[B_2H_7]^-$. Once $[B_2H_7]^-$ forms, it rapidly reacts with B_2H_6 (or BH_3) and converts to $[B_3H_8]^-$ in the presence of Ni nanoparticles. A similar mechanism has been proposed for the reaction between $[BH_4]^-$ and B_2H_6 to form $[B_3H_8]^-$, where $[BH_4]^-$ may donate one H^- to B_2H_6 forming $[B_2H_7]^-$ as the intermediate.[31]

In summary, we have demonstrated a new method to synthesize $Mg(B_3H_8)_2$ through the reaction between a Mg_2NiH_4/C composite and B_2H_6 gas. The reaction readily occurred at room temperature, which was accelerated by applying ball milling. *In situ* formed Ni or Ni_xB nanoparticles of 3–15 nm from the dissociation of Mg_2NiH_4 were considered to largely promote the formation of $Mg(B_3H_8)_2$. Furthermore, $MgB_{12}H_{12}$ formed on exposure of $Mg(B_3H_8)_2$ to B_2H_6.

This work was supported by the National Natural Science Foundation of China projects (no. 51431001, 51271078 and U120124), GDUPS (2014), Guangdong Natural Science Foundation (2014A030311004) and International Science & Technology Cooperation Program of China (2015DFA51750). Y. Yan and A. Remhof would like to acknowledge the financial support granted by Switzerland through the Swiss contribution to the enlarged European Union. The NMR hardware was

partially granted by the Swiss National Science Foundation (SNFS, grant no. 150638). Part of this work was based on collaboration facilitated by COST Action MP1103 "Nano-structured materials for solid-state hydrogen storage".

Notes and references

1 D. Y. Kim, Y. Yang, J. R. Abelson and G. S. Girolami, *Inorg. Chem.*, 2007, **46**, 9060–9066.
2 D. M. Goedde and G. S. Girolami, *J. Am. Chem. Soc.*, 2004, **126**, 12230–12231.
3 M. A. Toft, J. B. Leach, F. L. Himpsl and S. G. Shore, *Inorg. Chem.*, 1982, **21**, 1952–1957.
4 H. Beall and D. F. Gaines, *Inorg. Chim. Acta*, 1999, **289**, 1–10.
5 N. S. Hosmane and R. N. Grimes, *Inorg. Chem.*, 1980, **19**, 3482–3487.
6 Z. G. Huang, X. N. Chen, T. Yisgedu, J. C. Zhao and S. G. Shore, *Int. J. Hydrogen Energy*, 2011, **36**, 7038–7042.
7 Z. G. Huang, M. Eagles, S. Porter, E. G. Sorte, B. Billet, R. L. Corey, M. S. Conradi and J. C. Zhao, *Dalton Trans.*, 2013, **42**, 701–708.
8 M. Chong, A. Karkamkar, T. Autrey, S. Orimo, S. Jalisatgi and C. M. Jensen, *Chem. Commun.*, 2011, **47**, 1330–1332.
9 Y. Yan, A. Remhof, D. Rentsch, Y.-S. Lee, Y. Whan Cho and A. Zuttel, *Chem. Commun.*, 2013, **49**, 5234–5236.
10 Y. Yan, A. Remhof, D. Rentsch and A. Zuttel, *Chem. Commun.*, 2015, **51**, 700–702.
11 W. V. Hough, L. J. Edwards and A. D. McElroy, *J. Am. Chem. Soc.*, 1958, **80**, 1828–1829.
12 T. G. Hill, R. A. Godfroid, J. P. White and S. G. Shore, *Inorg. Chem.*, 1991, **30**, 2952–2954.
13 Z. G. Huang, G. King, X. N. Chen, J. Hoy, T. Yisgedu, H. K. Lingam, S. G. Shore, P. M. Woodward and J. C. Zhao, *Inorg. Chem.*, 2010, **49**, 8185–8187.
14 A. C. Dunbar, J. A. Macor and G. S. Girolami, *Inorg. Chem.*, 2014, **53**, 822–826.
15 Z. Huang, G. King, X. Chen, J. Hoy, T. Yisgedu, H. K. Lingam, S. G. Shore, P. M. Woodward and J.-C. Zhao, *Inorg. Chem.*, 2010, **49**, 8185–8187.
16 M. Chong, M. Matsuo, S. Orimo, T. Autrey and C. M. Jensen, *Inorg. Chem.*, 2015, **54**, 4120–4125.
17 O. Friedrichs, A. Remhof, A. Borgschulte, F. Buchter, S. I. Orimo and A. Zuttel, *Phys. Chem. Chem. Phys.*, 2010, **12**, 10919–10922.
18 A. Remhof, Y. Yan, D. Rentsch, A. Borgschulte, C. M. Jensen and A. Züttel, *J. Mater. Chem. A*, 2014, **2**, 7244–7249.
19 Y. Yan, Y. S. Au, D. Rentsch, A. Remhof, P. E. de Jongh and A. Zuttel, *J. Mater. Chem. A*, 2013, **1**, 11177–11183.
20 Y. S. Au, Y. Yan, K. P. de Jong, A. Remhof and P. E. de Jongh, *J. Phys. Chem. C*, 2014, **118**, 20832–20839.
21 M. Soderlund, P. Maki-Arvela, K. Eranen, T. Salmi, R. Rahkola and D. Y. Murzin, *Catal. Lett.*, 2005, **105**, 191–202.
22 P. V. Jasen, E. A. Gonzalez, G. Brizuela, O. A. Nagel, G. A. Gonzalez and A. Juan, *Int. J. Hydrogen Energy*, 2007, **32**, 4943–4948.
23 Y. G. Yan, A. Remhof, D. Rentsch and A. Zuttel, *Chem. Commun.*, 2015, **51**, 700–702.
24 P. Ngene, M. H. Verkuijlen, Q. Zheng, J. Kragten, P. J. M. van Bentum, J. H. Bitter and P. E. de Jongh, *Faraday Discuss.*, 2011, **151**, 47–58.
25 T. J. Carter, R. Mohtadi, T. S. Arthur, F. Mizuno, R. Zhang, S. Shirai and J. W. Kampf, *Angew. Chem., Int. Ed.*, 2014, **53**, 3173–3177.
26 R. M. Desrosiers, D. W. Greve and A. J. Gellman, *Surf. Sci.*, 1997, **382**, 35–48.
27 J. Xu, Y. Li, J. Cao, R. Meng, W. Wang and Z. Chen, *Catal. Sci. Technol.*, 2015, **5**, 1821–1828.
28 I. Saldan, S. Hino, T. D. Humphries, O. Zavorotynska, M. Chong, C. M. Jensen, S. Deledda and B. C. Hauback, *J. Phys. Chem. C*, 2014, **118**, 23376–23384.
29 J. J. Reilly and R. H. Wiswall, *Inorg. Chem.*, 1968, **7**, 2254–2256.
30 M. Zhu, Y. Lu, L. Ouyang and H. Wang, *Materials*, 2013, **6**, 4654.
31 D. F. Gaines, R. Schaeffer and F. Tebbe, *Inorg. Chem.*, 1963, **2**, 526–528.

